Korean Chem. Eng. Res., 53(3), 382-390 (2015)
http://dx.doi.org/10.9713/kcer.2015.53.3.382
PISSN 0304-128X, EISSN 2233-9558

Adsorption of Carbon Dioxide onto Tetraethylenepentamine Impregnated PMMA Sorbents with Different Pore Structure

Dong Hyun Jo, Cheonggi Park, Hyunchul Jung and Sung Hyun Kim†

Department of Chemical and Biological Engineering, Korea University, 145 Anam-ro, Seongbuk-gu, Seoul 136-701, Korea
(Received 4 August 2014; Received in revised form 14 October 2014; accepted 18 October 2014)

Abstract – Poly(methyl methacrylate) (PMMA) supports and amine additives were investigated to adsorb CO_2. PMMA supports were fabricated by using different ratio of pore forming agents (porogen) to control the BET specific surface area, pore volume and distribution. Toluene and xylene are used for porogens. Supported amine sorbents were prepared by wet impregnation of tetraethylenepentamine (TEPA) on PMMA supports. So we could identify the effect of the pore structure of supports and the quantity of impregnated TEPA on the adsorption capacity. The increased amount of toluene as pore foaming agent resulted in the decreased average pore diameter and the increased BET surface area. Polymer supports with huge different pore distribution could be fabricated by controlling the ratio of porogen. After impregnation, the support with micropore structure is supposed the pore blocking and filling effect so that it has low CO_2 capacity and kinetics due to the difficulty of diffusing. Macropore structure indicates fast adsorption capacity and low influence of amine loading. In case of support with mesopore, it has high performance of adsorption capacity and kinetics. So high surface area and meso-/macro- pore structure is suitable for CO_2 capture.

Key words: CO_2 Adsorption, Polymeric Support, Tetraethylenepentamine, Pore Distribution

1. Introduction

Global climate change has become a worldwide issue. Investigation of global climate change is considered to be one of the most critical point of research within the environmental emission control industry. Fossil fuels are the dominant form of energy utilized in the world and account for almost 75% of current CO_2 emissions [1]. These CO_2 emissions are one of the major causes of the increase in atmospheric temperature. Many suggested alternatives to reduce CO_2 emissions are the new and renewable energy, non-carbon energy resource like nuclear energy and energy efficiency improvement. Reducing the amount of warming gas is too much to select only one method and various technical plans should be used [2-4]. Therefore, thte application of carbon capture and storage (CCS) at fossil burning plants could considerably reduce the global emission of CO_2. The CCS technology has a potential which can reduce the energy cost and global warming gas.

The technology of CO_2 capture from combustion of fossil fuels could be separated into three parts: oxyfuel-combustion, pre-combustion, and post-combustion capture. The methods of post-combustion CO_2 capture are physical/chemical absorption, adsorption, membrane, oxygen-recovery and cryogenic process [5]. The commercial technology of CO_2 capture and separation required a great deal of energy expense and cost so that technological innovation is needed. For the capture of CO_2, the most popular technology is the sorption process using 'wet scrubbing' amine-based solution. But, this process has disadvantages such as solvent regeneration, high energy consumption, and the corrosion of the equipment and toxicity. A hopeful alternative technology to a liquid-phase sorption is a temperature or pressure swing adsorption system using the solid sorbents CO_2 capture [6-9]. It offers energy saving and stable performance. Porous supports such as activated carbons, zeolites, silica, alumina, and polymer are good materials for capturing CO_2 [10-14]. Compared to the wet-type adsorption process, dry-type is expected to reduce hazardous material and have low corrosion of equipment. Also, it has the advantage of overcoming high energy expense when the adsorbent is recycled. It needs more time to commercialize, but CO_2 capture by solid amine sorbents has been an increasingly active area of research.

Among the various dry-type solid sorbents, porous polymer support is employed used for low temperature use. Zeolites, silica, and alumina type have high surface area and thermal stability, but high cost. In case of activated carbon, it has the advantage of low cost and highest surface area, but has difficulty of pore size selection and problems of porosity control on account of very small pore size below 2 nm [15]. Porous polymer support as solid sorbent for low temperature use is able to increase the stability by cross-linking control and regenerate at low temperature. It also has low cost, a simple manufacturing process compared with inorganic supports, and several factors for commercialization [16]. While solid sorbents like zeolite and activated carbons have the property of reducing CO_2 capture capacity in a presence of water vapor, amine-impregnated porous polymer support increases it. And additional dehydration process is not

† To whom correspondence should be addressed.
E-mail: kimsh@korea.ac.kr
‡This article is dedicated to Prof. Seong-Youl Bae on the occasion of his retirement from Hanyang University.

needed [17,18]. The structure of the support plays an important role in sorbent performance. In general, large pore size tends to improve sorbent capacity. To further improve the performance of amine-functionalized porous sorbent, significant efforts have been directed towards developing the optimum support structure. Pore size and distribution is very significant for impregnating the amine and defusing the CO_2 at supported amine sorbents, so it relates to CO_2 adsorption capacity directly [19].

A variety of research on support such as silica or zeolite has been carried out for capturing CO_2 until now. However, the part of polymer support has not proceeded. It is essential to find the optimal structure for manufacturing suitable solid sorbent. Polymer support can change the structure easily by tuning variables. It is also able to control the porosity and pore size using pore foaming agent (porogen) during the synthesis. Through the control of porogen, optimal selective pore structure can be fabricated for capturing CO_2. Supported amine sorbents consist of a high surface area support with amine functional group grafted to its surface. Amine functional groups have been used to capture CO_2 in the province of wet and dry type adsorption process widely. Tetraethylenepentamine (TEPA) was used for functional amine group by wet-impregnation in this study. This study focuses on fabricating the PMMA supports with different pore size distribution followed by their impregnation with tetraethylenepentamine. The obtained samples were characterized by thermogravimetric analysis (TGA) to find the optimal pore structure.

2. Experimental

2-1. Materials

Methyl methacrylate (MMA) and ethylene glycol dimethacrylate (EGDMA) as monomer and toluene and xylene as pore foaming agent (porogen) were purchased from Sigma-Aldrich. Hydroxyethyl cellulose and benzoyl peroxide were purchased from Tokyo Chemical Industry. Methanol, tetraethylenepentamine (TEPA), HP-2MG (Mitsubishi Co. Ltd., Tokyo, Japan) were purchased from Sigma-Aldrich. Monomers were used after purification to remove inhibitor. All of supports were extracted with methanol for 10 h and dried for 8 h under vacuum at 353 K before use.

2-2. Method

2.2.1 Synthesis of porous PMMA

Fabricated porous acrylic ester resin beads were prepared by suspension polymerization. In a typical procedure, an aqueous phase (450 g) composed of 0.9 g of hydroxyethyl cellulose as dispersing agent was prepared separately. An organic phase (150 g) was composed of 75 g of monomer (25 g of methyl methacrylate and 50 g of ethylene glycol dimethacrylate) and 75 g of pore foaming agent (porogen) of different ratio of toluene and xylene. Benzoyl peroxide (1 wt% relative to monomer) was added to the organic phase. Prior to use, both the aqueous and organic phase were purged with N_2 for 5 min. The aqueous phase was added to 1000 mL parallel-sided flanged gastight round-bottom flask with a metal stirrer carrying two impellers and followed by the organic phase under N_2 condition. The suspension polymerization was kept at 353 K for 10 h under N_2 to complete the polymerization, and the stirring speed was set to be 400 rpm. The beads were filtered using a 75 μm sieve. The filtered beads were washed with aqueous methanol (20%, 1000 mL) and extracted with acetone in a Soxhlet apparatus for 10 h, and dried under vacuum at 313 K for 10 h. The resulting beads were fractionated to size of 106 μm and 425 μm for the experiments. The samples obtained were denoted as T-x, where x represents the concentration of toluene as pore foaming agent.

2-2-2. Amine Impregnation

The adsorbent impregnated tetraethylenepentamine (TEPA) was prepared by physical impregnation of porous poly(methyl methacrylate) supports (synthesized polymer): the ratio of toluene as porogen 0%, 50%, and 100%. Physical impregnation is the method of wet impregnation without chemical reaction between support and functional group. TEPA was dissolved in methanol completely and mixed with porous support beads in a round bottom flask. The impregnation was kept at 348 K for 6 h to evaporate methanol. After impregnation, TEPA was dispersed on the internal and external surface of the porous PMMA supports. TEPA-impregnated sorbent was dried at 358 K for 8 h completely before use. The amine loading was controlled by adjusting the ratio of amine and methanol. In this study, amine loadings were 30 wt%, 40 wt%, and 46 wt% based on preliminary research, respectively. The samples were denoted as T-x/(y)T, where x represents the ratio of toluene as pore foaming agent and (y)T represents the condition of TEPA impregnation on supports; (y) is the amount of TEPA loading.

2-2-3. Characteristics of supports

The surface area was estimated by using the Brunauer, Emmett, and Teller (BET) equation [20] based on information obtained by N_2 adsorption and desorption at 77 K using a volumetric sorption analyzer (Autosorb iQ Station 2, Quantachorme), and the pore diameter, volume and size distribution was analyzed. Fourier transform infrared spectroscopy (FT-IR) of porous PMMA resins was compared with commercial acrylic ester resin, HP-2MG to confirm the fabricated polymer through a peak comparison. The surface morphology of supports was analyzed by scanning electron microscope (SEM).

2-3. Adsorption and Desorption energy

A thermogravimetric analyzer (TGA) was used to analyze the adsorption and desorption performance of the prepared adsorbents. In a typical experiment, around 15 mg of adsorbent was placed inside the TGA furnace. The sample was heated up to 80 ^{o}C in the flow of 60 mL of high purity N_2 to desorb the pre-adsorbed impurities, CO_2 and moisture. The temperature was kept constant until the sample mass stabilized. Then, the sample was cooled to the desired adsorption temperature (35 ^{o}C, 70 ^{o}C). The equilibrium adsorption experiments

of four kinds of porous PMMA supports with different pore size distribution were at 35 °C. The desorption temperature and energy was analyzed by temperature programmed desorption. Saturated adsorbent was heated to desorb the CO_2 and both desorption temperature and energy were measured.

3. Results and Discussion

3-1. Characterization of porous PMMA adsorbent

Many pore foaming agents (porogen) such as toluene, cyclohexane, and xylene are used to make porous material. We used toluene and xylene to fabricate porous acrylic ester polymer with huge different pore size distribution. Porous poly(methyl methacrylate) supports with the ratio of toluene 0%, 50%, and 100% were synthesized by controlling the pore foaming agent and compared with commercial polymer, HP-2MG. The properties of support samples were analyzed by BET equipment.

The FT-IR spectra of HP-2MG support and three samples, i.e., T-0, T-50, and T-100, are shown in Fig. 1. The spectra of all of the powdered samples were recorded by FT-IR spectrometer without any pretreatment. All poly(methyl methacrylate) supports exhibited rather similar spectra. The characteristic peaks of carbonyl and acetyl groups at 1740 cm^{-1} and ester group at 1150 cm^{-1} indicate that the four resins are all acrylic ester polymers. From this, manufactured supports confirmed the poly(methyl methacrylate) polymer by comparing with HP-2MG.

By changing the ratio of toluene as porogen in preparing the porous supports, a series of samples with different pore structures were obtained. Fig. 2 shows the morphology of four samples: HP-2MG, T-0, T-50, and T-100. The image of surface of HP-2MG was similar to T-50 and

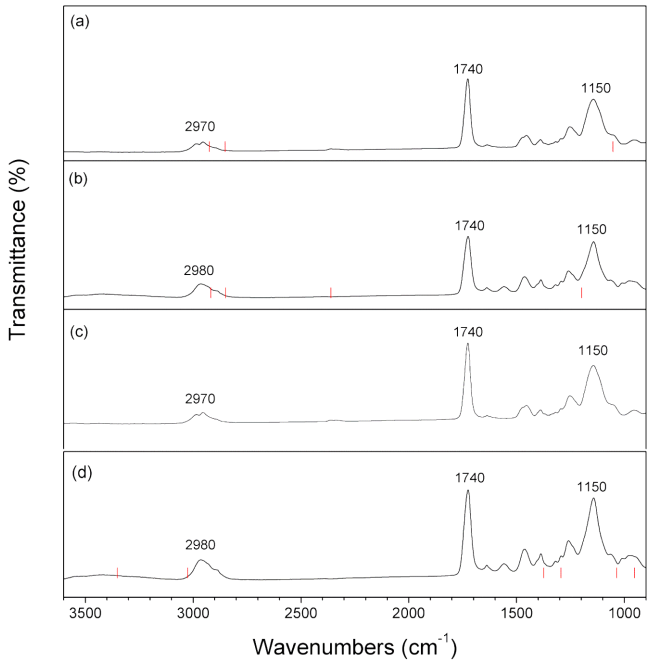

Fig. 1. FT-IR of four acrylic resins (HP-2MG, T-0, T-50 and T-100). (a) HP-2MG, (b) T-0, (c) T-50, (d) T-100.

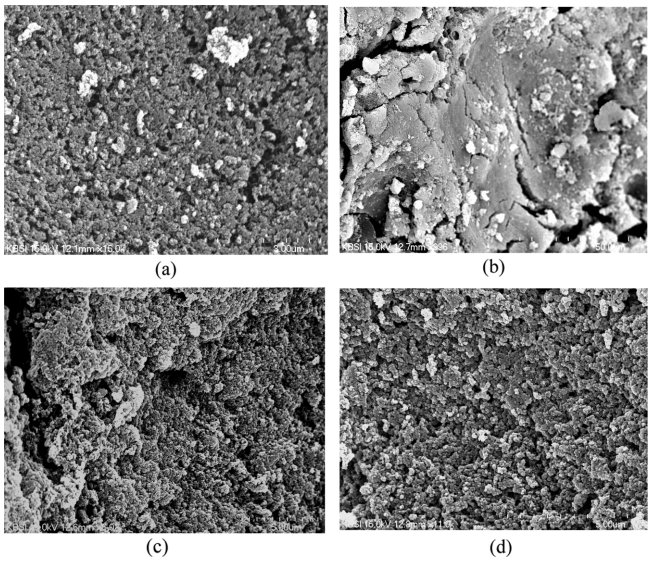

Fig. 2. Surface morphology of four PMMA supports. (a) HP-2MG, (b) T-0, (c) T-50, (d) T-100.

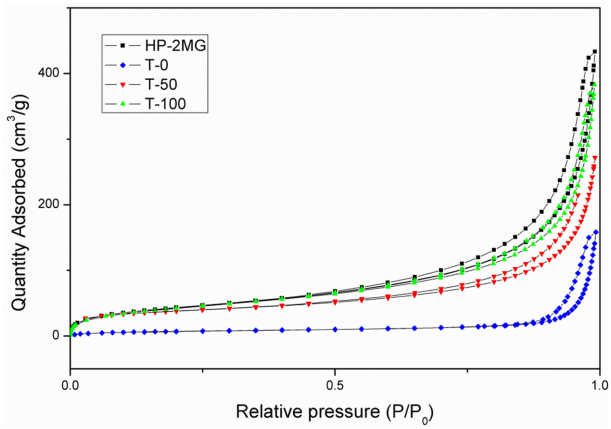

Fig. 3. Nitrogen adsorption and desorption isotherm of HP-2MG, T-0, T-50 and T-100.

T-100 with porous property. T-0 had the image of smooth surface and slight pores, relatively. The BET analysis needs to be performed for precise porosity examination.

The N_2 adsorption and desorption isotherms of HP-2MG, T-0, T-50, and T-100 are shown in Fig. 3, which indicates the typical type IV isotherm shape with mesopore areas. In case of T-0, the N_2 gas was not adsorbed at the region of micro- and mesopores. T-0 is supposed to have macropore structure. The type of N_2 adsorption and desorption is physical adsorption that is greatly influenced by pore structure. Table 1 compares the properties of three fabricated porous supports with commercial polymer, HP-2MG. The T-0, T-50, and T-100 have the BET surface area of 371.09 m^2/g, 425.61 m^2/g, and 525.08 m^2/g, respectively. It also had the micropore surface area of 1.25 m^2/g, 101.23 m^2/g, and 258.81 m^2/g, respectively. From this, we confirmed that the increased amount of toluene as pore foaming agent makes the micropore surface area larger. Micropore surface area is closely related to total BET surface area. Ultimately, the increased microp-

Table 1. Structure property of the unmodified and amine-modified PMMA supports

Samples	BET surface area (m^2/g)	Pore volume (cm^3/g)	Pore diameter peak (nm)
Pure support (unmodified)			
HP-2MG	614.65	1.00	39.97
T-0	371.09	2.18	80.83
T-50	425.61	0.83	24.41
T-100	525.08	0.75	8.80
Amine-modified adsorbent (different amine loading)			
HP-2MG/(30)T	225.75	0.80	44.47
T-0/(30)T	190.32	1.27	75.08
T-50/(30)T	201.46	0.69	39.27
T-100/(30)T	82.52	0.41	44.90
HP-2MG/(40)T	180.39	0.62	51.35
T-0/(40)T	170.23	0.94	68.99
T-50/(40)T	161.39	0.56	47.28
T-100/(40)T	27.19	0.23	39.30
HP-2MG/(46)T	61.17	0.49	65.81
T-0/(46)T	89.64	0.70	58.62
T-50/(46)T	50.07	0.41	63.74
T-100/(46)T	19.84	0.21	30.01

ore surface area results in the increased total BET surface area and the decreased pore size and volume, so that it shows to trade off pore size and volume against surface area.

Four samples were impregnated with amine to make a supported amine sorbent. Table 1 also shows the result of BET analysis for the supported TEPA sorbents with different TEPA loading: 30 wt%, 40 wt%, 46 wt%, respectively. All of the amine-modified adsorbents show the decreased BET surface area and pore volumes. The BET surface area of T-100/T with micropore structure decreased from 525.08 m^2/g to 82.52 m^2/g (30 wt%), 27.19 m^2/g (40 wt%), 19.84 m^2/g (46 wt%), and the pore volume of T-100/T decreased from 0.75 cm^3/g to 0.41 cm^3/g (30 wt%), 0.23 cm^3/g (40 wt%), 0.21 cm^3/g (46 wt%) after TEPA impregnation, respectively. Most of supports with micropore structure lose the micropore surface area below 2 nm after impregnation of amine. It is supposed the pore block and filling effects at micropore structure. T-0 with macropore structure had a little micropore after TEPA impregnation.

Fig. 4 shows the peak of pore-size distribution shifts to the left with increase of the ratio of toluene, generally. It seems that the tolu-

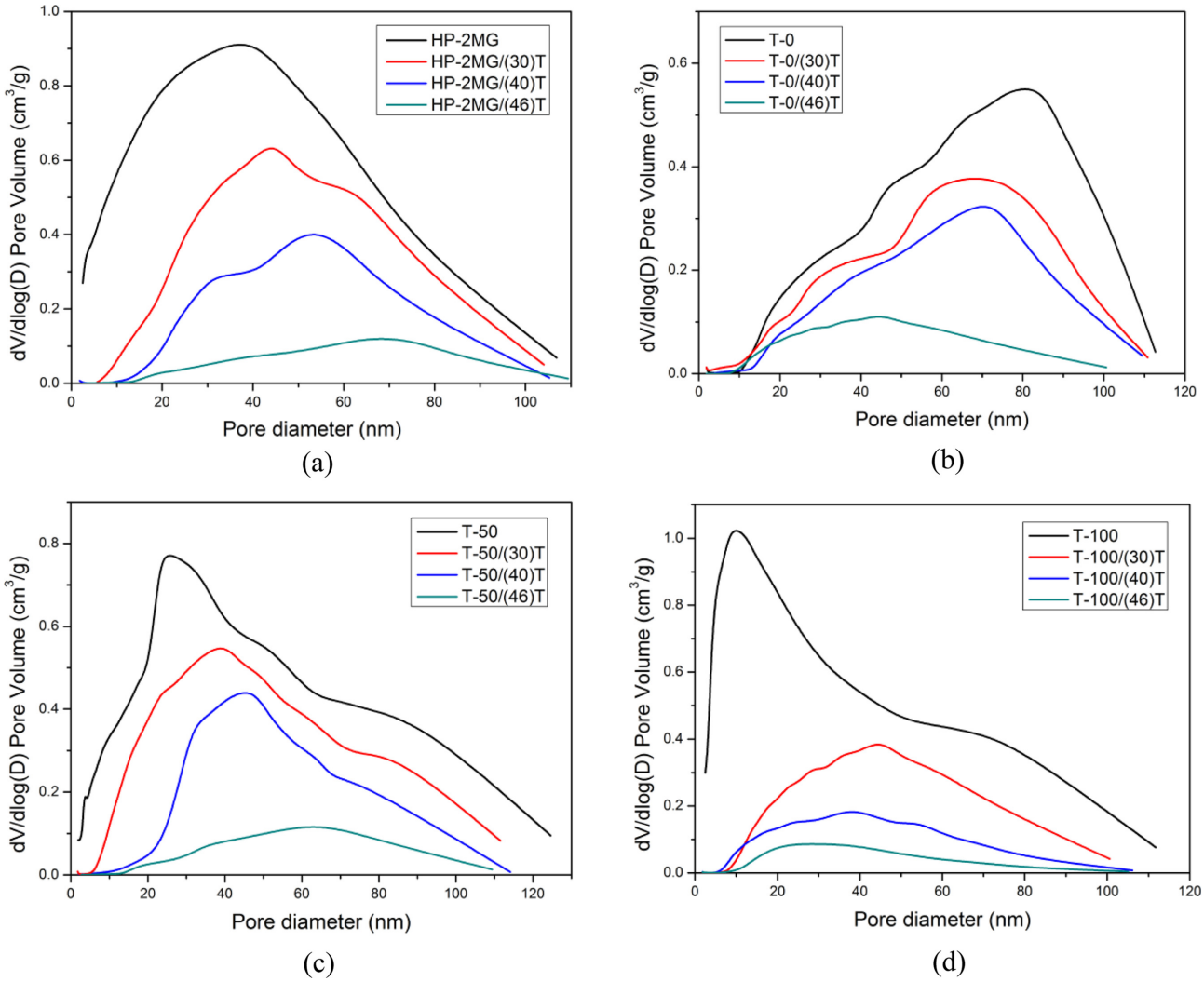

Fig. 4. Pore distribution curves of amine-modified adsorbent with different amine loading (a) HP-2MG, (b) T-0, (c) T-50, and (d) T-100.

ene as porogen develops a micropore structure. And commercial porous PMMA polymer, HP-2MG, has mesopore size of 2~50 nm, and its characteristics are similar to T-50. Fig. 4 also shows the pore-size distribution of TEPA-modified adsorbents with different TEPA loading, which clearly indicates that the loaded TEPA was filled into the pores and resulted in the significant reduction of the pore volume and surface area. Interestingly, the increase of the TEPA loading amount reduced the pore volume, but not significantly changed the pore size. Instead, as shown in Table 1, the increased amine loading resulted in the increased pore diameter peak. This is probably because the micropore structure was firstly filled with amine functional group. We could identify the pore block and filling effects in Fig. 4. Specific micropore area also could not be measured by BET analysis because it does not exist. The micropore area of pure supports was blocked by amine-functional groups, even in case of 30 wt% impregnation.

3-2. CO_2 adsorption dynamics and capacity of amine-modified PMMA supports

3-2-1. Screening test for operating temperature

For practical CO_2 capture, the adsorbents should not only have high sorption capacity, but also possess high adsorption/desorption rates and stable regeneration performance. To be energy-efficient, the adsorption and desorption of CO_2 must be fast. In general, solid amine sorbents have high adsorption/desorption rates due to the high gas/sorbents interface area. In this part, a screening test was carried out for operating temperature. Fig. 5 shows that CO_2 adsorption dynamics and capacity were measured at different temperature (35 °C and 70 °C) by TGA. Usually, porous polymer support has a high adsorption capacity at lower temperature due to the property of physical adsorption. While the adsorption capacity at 35 °C is higher than that at 70 °C, the initial adsorption rate is almost the same. Therefore, the operating temperature was set of 35 °C. To investigate the effect of textural properties of support and temperature on CO_2 adsorption capacity, the relationship of CO_2 adsorption capacity

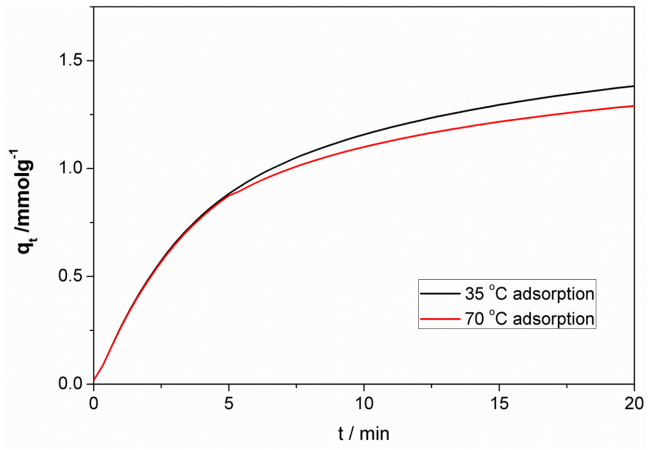

Fig. 5. Breakthrough curves of CO_2 for supported amine sorbents (HP-2MG/(40)T) at different temperature over time (99.999 vol% CO_2).

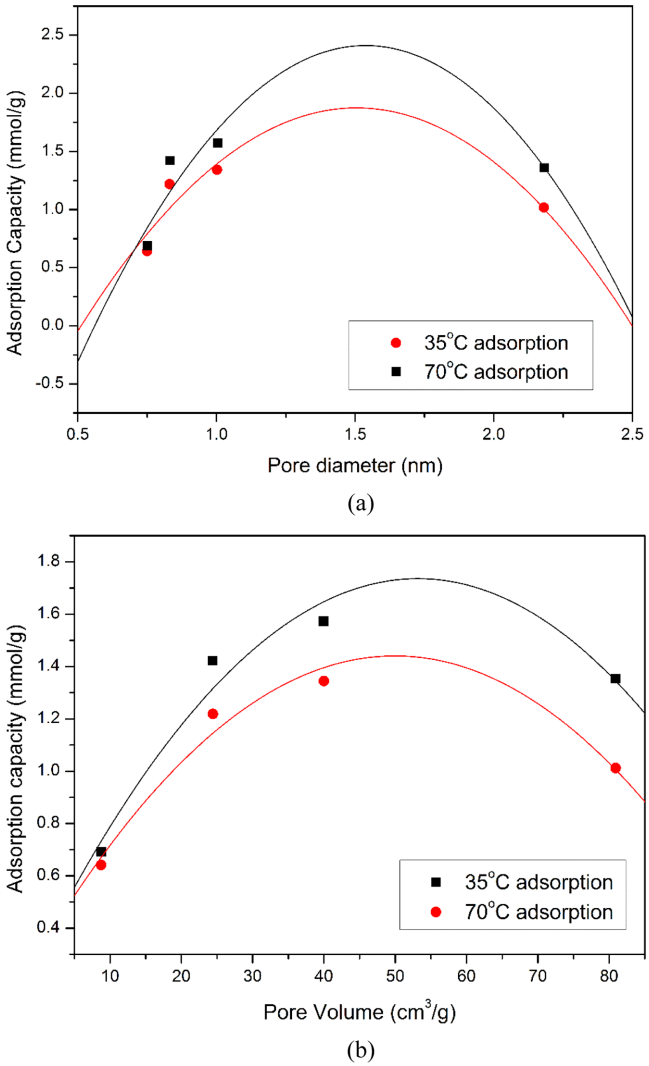

Fig. 6. Relationship between the pore structure of substrate and CO_2 capture capacity at different temperature.

versus the values of pore volume and pore diameter was plotted at 35 °C and 70 °C in Fig. 6(a) and Fig. 6(b), respectively. The second-order polynomial fitting is used to predict unmeasured point ($y = \text{Intercept} + B1*x^1 + B2*x^2$). When CO_2 adsorbed sorbent was regenerated by TSA process, N_2 purge gas was usually used to increase the diffusivity in lab scale test. However, this method is not suitable in a real regenerating process. The reason is that the mixture of captured CO_2 and N_2 purge gas needs to separate for dilute gas so that the additional operating equipment and costs will occur. Therefore, high purity CO_2 should be used for purge gas. In Fig. 6(a) and Fig. 6(b), the difference of adsorption capacity between two temperature point indicates the cyclic capacity in real process. From this, the optimum pore volume and pore diameter are about 1.5 cm^3/g and 55 nm, respectively.

3-2-2. CO_2 adsorption dynamics and capacity

The breakthrough curves of the CO_2 adsorption on various PMMA supports with different quantities of impregnated TEPA are shown in

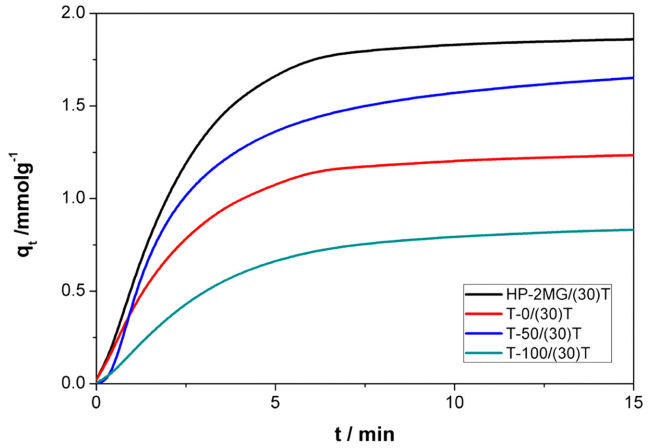

(a) TEPA 30 wt% loading

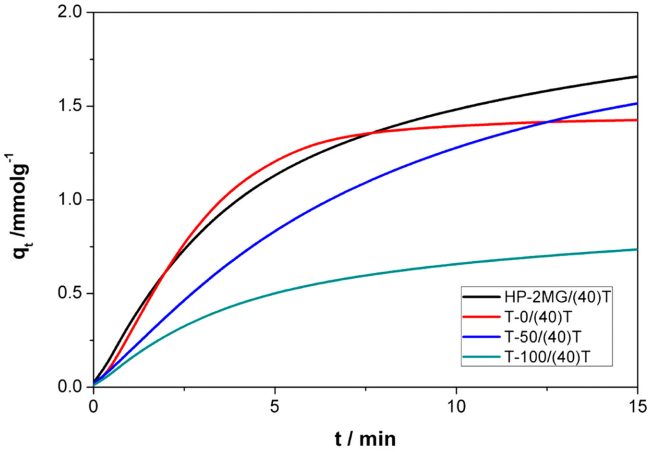

(b) TEPA 40 wt% loading

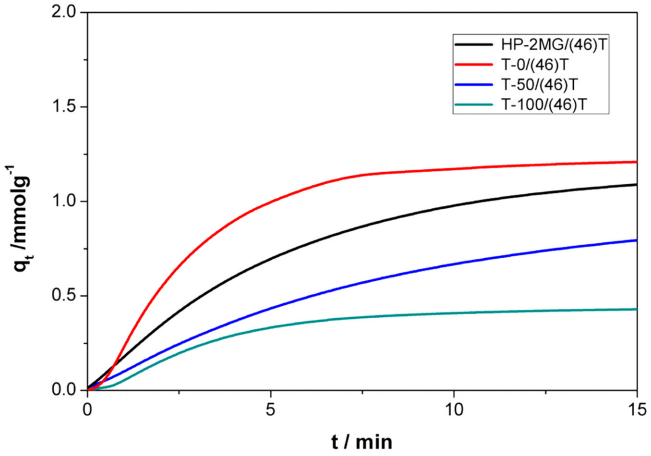

(c) TEPA 46 wt% loading

Fig. 7. Breakthrough curves of CO_2 for supported amine sorbents with different pore structure over time (99.999 vol% CO_2, 35 °C).

Figs. 7 and 8. From the inset image of the partial enlargement, when the quantity of impregnated TEPA is 30 wt% loading in Fig. 7(a), the breakthrough curves are similar to each other. The supports of HP-2MG and T-50 with mesopore structure show better performance than the other supports. In case of sorbent of T-100/(30)T with micropore structure, it was estimated the pore block and filling proceeded in terms of micropore structure from the low adsorption rates, capacity and previous BET analysis. So it resulted in a decreased accessibility of the amine groups inside the particle, resulting in a lower effective CO_2 capacity of adsorption. From this, TEPA-impregnated adsorbent with a micropore support loses the porous properties. At low amine loading, the porosity is relatively large and hence there is small resistance for CO_2 transfer. T-0/(40)T of 40 wt% impregnated TEPA in Fig. 7(b) indicated the fastest adsorption rate due to ease of diffusing the CO_2 into inner pores. The mesopore TEPA-modified adsorbents of HP-2MG/(40)T and T-50/(40)T appear as fast adsorption rate and highest adsorption capacity. As the quantity of impregnated TEPA is 46 wt% as excess amount, the sorbent of T-0/(46)T with macropore structure reversed it of HP-2MG and T-50 with mesopore structure in terms of the dynamics and capacity. The sorbents with mesopore structure also proceeded the pore block and filling effect.

Adsorption rate constant was predicted by the second-order models to perform the precise analysis with the expressions in either of the following Eqs. (1) and (2) [21].

$$\frac{dq_t}{dt} = k(q_e - q_t)^2 \quad (1)$$

$$\frac{t}{q_t} = \frac{1}{kq_e^2} + \frac{1}{q_e}t \quad (2)$$

where q_e and q_t (mmol·g^{-1}) are the CO_2 adsorption saturated capacities and the adsorption capacities at time t, respectively; k (mmol/g·min)$^{-1}$ is the rate constant of a second-order adsorption [22].

In Eq. (2), the plots of (t/q_t) against t for TEPA-modified adsorbents have a meaningful linear relationship. The adsorption rate is proportional to the square of the free adsorption sites. The conclusion perfectly corresponds with the proposal of the CO_2 adsorption mechanism, that for one CO_2 molecule, two active sites, such as –NH_2 groups, or one -NH_2 group and one -OH group, are needed to complete the adsorption. The saturated adsorption capacity q_e and the rate constant k can be calculated by the intercept and slope of the fitting lines. As shown in Table 2, the adsorption rate constant obviously decreases with an increase in the quantity of impregnated TEPA due to the blocking of TEPA in the pores of supports, and the corresponding CO_2 diffusion resistance in sorbents increases. It also decreases with a decreases in pore diameter and volume in 40 and 46 wt% TEPA loading. HP-2MG/(30)T and T-50/(30)T of the low TEPA loading with mesopore structure has relatively high rate constant of 0.071 and 0.058 (min g/mmol). The effects of the pore structure of supports and the quantity of impregnated TEPA on the saturated adsorption capacity q_e coincide with the predicted and experimental results in Fig. 7 and Table 2 quite well. Fig. 8 is another expression of kinetics in terms of the quantity of impregnated TEPA in fixed support to analyze the effect of amine loading easily. All of the adsorbents excepting T-0 support show that the increased amine loading resulted in the decreased adsorption capacity and kinetics. T-0 support with macropore structure has a large pore diameter and volume

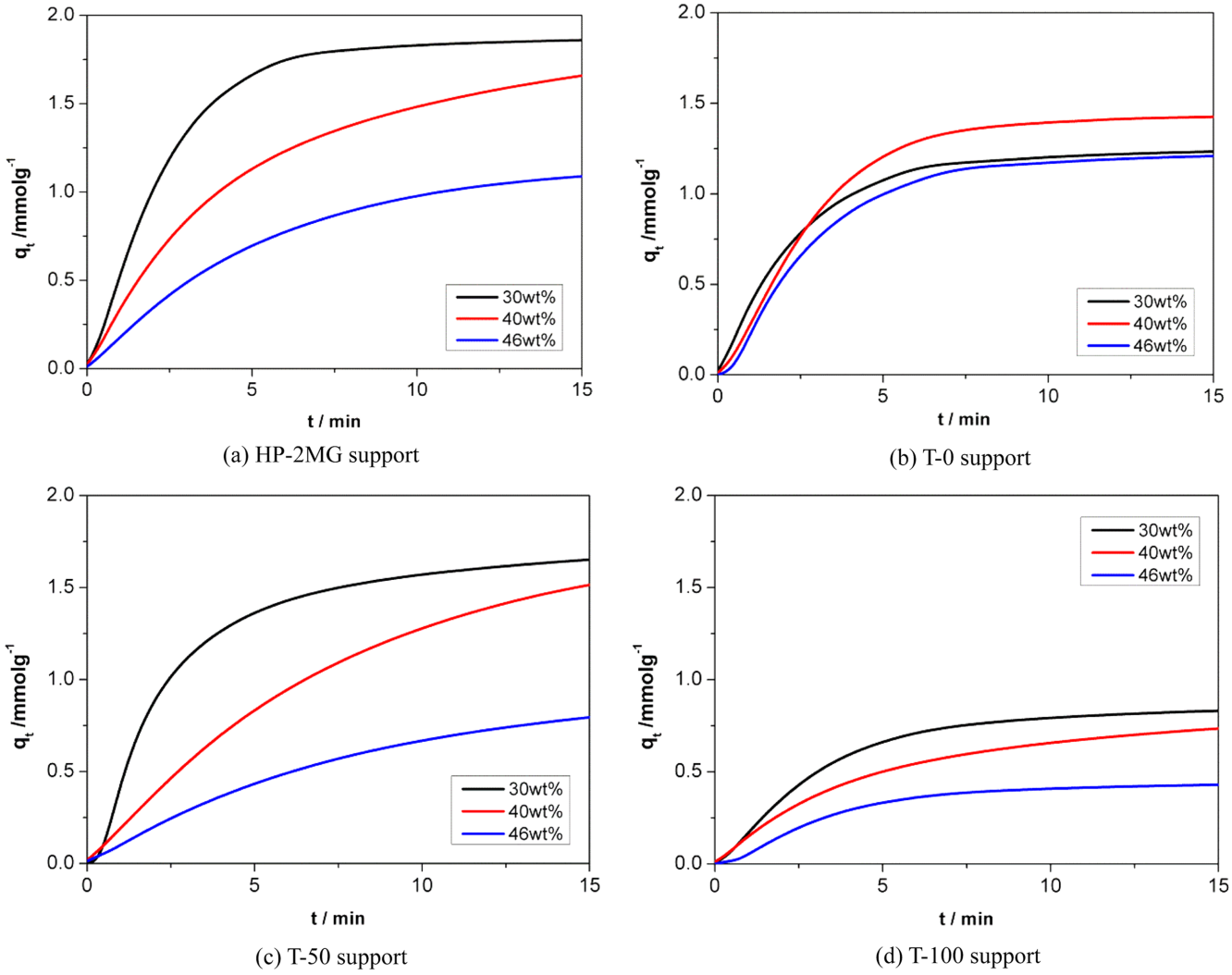

(a) HP-2MG support (b) T-0 support

(c) T-50 support (d) T-100 support

Fig. 8. Breakthrough curves of CO_2 for supported amine sorbents with different amine loading over time (99.999 vol% CO_2, 35 °C).

Table 2. The fitting parameters of the equilibrium adsorption capacity q_e and the rate constant k by Eq. (2)

Samples	Capacity (mmol/g)	Saturated capacity (mmol/g)	Rate constant k (mmol/g)·min)$^{-1}$
HP-2MG/(30)T	1.92	2.01	0.071
T-0/(30)T	1.28	1.35	0.041
T-50/(30)T	1.87	1.98	0.058
T-100/(30)T	0.94	1.09	0.013
HP-2MG/(40)T	2.16	2.30	0.048
T-0/(40)T	1.49	1.54	0.050
T-50/(40)T	1.95	2.12	0.038
T-100/(40)T	0.69	0.87	0.009
HP-2MG/(46)T	1.27	1.42	0.020
T-0/(46)T	1.35	1.50	0.032
T-50/(46)T	1.04	1.28	0.011
T-100/(46)T	0.60	0.70	0.007

enough to diffuse the CO_2 molecules after impregnation so that all of the TEPA-modified adsorbents (30, 40, and 46 wt%) have similar adsorption kinetics.

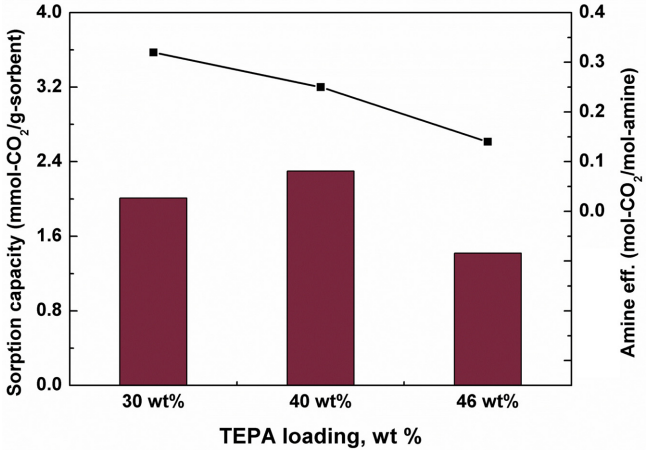

Fig. 9. Effect of different TEPA loading on the CO_2 sorption capacity and amine efficiency.

3-3. Amine efficiency and desorption energy

The efficiency of the amine groups in the loaded TEPA is defined as a molar ratio of the adsorbed CO_2 to the amine groups in the sorbent as the support using HP-2MG, representatively, and the result is

Table 3. Adsorption and desorption characteristics of TEPA-modified adsorbents by TPD. Desorption peak temperature was calculated with heating rate of 10 K/min

Samples	Desorption peak Temperature (°C)	Desorption energy (kJ/mol)
HP-2MG/(30)T	90	41.56
T-0/(30)T	68	35.61
T-50/(30)T	89	41.33
T-100/(30)T	92	42.08
HP-2MG/(40)T	97	42.20
T-0/(40)T	74	37.54
T-50/(40)T	90	41.70
T-100/(40)T	*	*
HP-2MG/(46)T	98	42.54
T-0/(46)T	77	38.82
T-50/(46)T	93	42.15
T-100/(46)T	*	*

*:unmeasured point

shown in Fig. 9. Although the adsorption capacity is highest at 40 wt% TEPA loading, the amine efficiency has better performance at 30 wt% TEPA loading. The reason is the reduction of the percentage of the accessible amine sites due to increase of the diffusion resistance of CO_2 into the bulk TEPA in the pores.

The CO_2 desorption property of TEPA-modified adsorbent was measured by temperature programmed desorption (TPD) and the results are shown in Table 3. For analysis of the desorption property, T-100(40)T and T-100(46)T were excluded due to poor CO_2 adsorption capacity. Desorption energy can be calculated by Amenomiya equation (Eq. (3)).

$$\log\left(\frac{T_P^2}{\beta}\right) = \frac{E_d}{2.303RT_p} + \log\left(\frac{E_d A_0}{RC}\right) \quad (3)$$

where T_P is desorption peak temperature (K), β is heating rate (K/min), E_d is energy of desorption (kJ/mol), A_0 is quantity absorbed, and C is constant related to desorption rate [23]. Difference in heating rate shifts desorption peak temperature. The plots of $\log(T_P^2/\beta)$ against $1/T_P$ have a significant linear relationship so that desorption energy can be calculated by the slope. As expected, desorption peak temperature and desorption energy decreased with increasing pore size and decreasing amine loading. Desorption characteristics are similar between HP-2MG and T-50 with mesopore structure. These were with a little higher desorption temperature than support with macropore structure, but had one-and-a-half adsorption capacity. The support with mesopore structure is a better adsorbent than it is with macropore structure. In case of support with micropore structure, the amount of adsorption is too small to identify desorption properties by blocking and filling of support pores. It cannot perform a role as adsorbent effectively due to losing porosity. The supports with mesopore and macropore structure maintain porous property after amine impregnation without pore blocking and can be effective adsorbent on this account.

4. Conclusion

Commercial porous PMMA support HP-2MG and three fabricated polymer with different porous properties were prepared and impregnated with 30 wt%, 40 wt%, and 46 wt% TEPA for CO_2 capture. Supported amine sorbents were tested experimentally for application in post-combustion CO_2 capture.

The sorption CO_2 capacity of adsorbent was a strong function of pore properties as surface area, pore diameter and volume. Significant improvement of the sorption capacity was achieved by tuning these variables. The amine functional group impregnated micropore adsorbent has low sorption capacity due to blocking and filling of support pores. Solid sorbent with macropore structure has fast adsorption kinetics and low influence of amine loading. Adsorbents with mesopore diameter and volume show better performance in terms of CO_2 adsorption/desorption capacity and kinetics. PMMA support, which has similar property with commercial polymer, could be fabricated. Furthermore, suitable polymer support for capturing CO_2 is able to be manufactured by controlling the pore structure unlike commercial support.

Acknowledgments

This work was supported by the Korea CCS R Center (KCRC) grant funded by the Korea government (Ministry of Science, ICT & Future Planning) (no. NRF-2014M1A8A1049251).

References

1. Kim, Y., Ryu, J. and Lee, I., "Recent Research Trends of Chemical absorption in CCS (Carbon dioxide Capture and Storage) and the role of Process Systems Engineering," *Korean Chem Eng. Res*., **47**, 531-537(2009).
2. Konduru, N., Lindner, P. and Assaf-Anid, N., "Curbing the Greenhouse Effect by Carbon Dioxide Adsorption with Zeolite 13X," *AIChE J*., **53**, 3137-3143(2007).
3. Song. C., "Global Challenges and Strategies for Control, Conversion and Utilization of CO_2 for Sustainable Development Involving Energy, Catalysis, Adsorption and Chemical Processing," *Catal. Today*, **115**, 2-32(2006).
4. Haszeldine, R. S., "Carbon Capture and Storage: How Green Can Black Be?," *Science*, **325**, 1647-1652(2009).
5. Aaron, D. and Tsouris, C., "Separation of CO_2 from Flue Gas: A Review," *Sep. Sci. Technol*., **40**, 321-348(2005).
6. Hao, G. P., Li, W. C. and Lu, A. H., "Novel Porous Solids for Carbon Dioxide Capture," *J. Mater. Chem*., **21**, 6447-6451(2011).
7. Jo, D. H., Cho, K. S., Park C. G. and Kim. S. H., "Effects of Inorganic-organic Additives on CO_2 Adsorption of Activated Carbon," *Korean Chem Eng. Res*., **50**, 885-889(2012).
8. Hong, M. S., Pankaj, S., Jung, Y. H., Park, S. Y., Park, S. J. and Baek, I. H., "Separation of Carbon Dioxide Using Pelletized Zeolite Adsorbent with Amine Impregration," *Korean Chem. Eng. Res*., **50**, 244-250(2012).
9. Yi, C., "Advances of Post-Combustion Carbon Capture Technology by

Dry Sorbent," *Korean Chem. Eng. Res*., **48**(2), 140-146(2010).
10. Reynolds, S. P., Ebner, A. D. and Ritter, J. A., "Carbon Dioxide Capture from Flue Gas by Pressure Swing Adsorption at High Temperature Using a K-promoted HTlc: Effects of Mass Transfer on the Process Performance," *Environ. Prog*., **25**, 334-342(2006).
11. Gomes, V. G. and Yee, K. W. K., "Pressure Swing Adsorption for Carbon Dioxide Sequestration from Exhaust Gases," *Sep. Purif. Technol*., **28**, 161-171(2006).
12. Sebastian, V., Kumakiri, I., Bredesen, R. and Menendez, M., "Zeolite Membrane for CO_2 Removal: Operating at High Pressure," *J. Memb. Sci*., **292**, 92-97(2007).
13. Ma, S. and Zhou, H. C., "Gas Storage in Porous Metal-organic Frameworks for Clean Energy Applications," *Chem. Commun. (Camb)*, **46**, 44-53(2010).
14. Siriwardane, R. V., Shen, M. S., Fisher, E. P. and Poston, J. A., "Adsorption of CO_2 on Molecular Sieves and Activated Carbon," *Energy Fuels*, **15**, 279-284(2001).
15. Houshmand, A., Daud, W. M. A. W., Lee, M. G. and Shafeeyan, M. S., "Carbon Dioxide Capture with Amine-Grafted Activated Carbon," *Water, Air, Soil Pollut*., **223**, 827-835(2011).
16. Gray, M. L., Hoffman, J. S., Hreha, D. C., Fauth, D. J., Hedges, S. W., Champagne, K. J. and Pennline, H. W., "Parametric Study of Solid Amine Sorbents for the Capture of Carbon Dioxide," *Energy Fuels*, **23**, 4840-4844(2009).
17. Xu, X., Song, C., Miller, B. G. and Scaroni, A.W., "Influence of Moisture on CO_2 Separation from Gas Mixture by a Nanoporous Adsorbent Based on Polyethylenimine-Modified Molecular Sieve MCM-41," *Ind. Eng. Chem. Res*., **44**, 8113-8119(2005).
18. Bhagiyalakshmi, M., Yun, L. J., Anuradha, R. and Jang, H. T., "Synthesis of Chloropropylamine Grafted Mesoporous MCM-41, MCM-48 and SBA-15 from Rice Husk Ash: Their Application to CO_2 Chemisorption," *J. Porous Mater*., **17**, 475-484(2009).
19. Chen, C., Yang, S. T., Ahn, W. S. and Ryoo, R., "Amine-impregNated Silica Monolith with a Hierarchical Pore Structure: Enhancement of CO_2 Capture Capacity," *Chem. Commun. (Camb)*, **24**, 3627-3629(2009).
20. Adharapurapu, R. R., Kumar, D., Zhu, J., Torbet, C. J., Was, G. S. and Pollock, T. M., "Chromia-Assisted Decarburization of W-Rich Ni-Based Alloys in Impure Helium at 1273 K (1000 ^{o}C)," *Metall. Mater. Trans. A*., **42**, 1229-1244(2010).
21. Ho, Y. S., "Review of Second-order Models for Adsorption Systems," *J. Hazard. Mater*., **136**, 681-689(2006).
22. Yan, W., Tang, J., Bian, Z., Hu, J. and Liu, H., "Carbon Dioxide Capture by Amine-Impregnated Mesocellular-Foam-Containing Template," *Ind. Eng. Chem. Res*., **51**, 3653-3662(2012).
23. Cvetanović, R. J. and Amenomiya, Y., "Application of a Temperature-Programmed Desorption Technique to Catalyst Studies," *Adv. Catal*., **17**, 103-149(1967).